Structural Engineering and Mechanics, *Vol. 64, No. 1 (2017) 93-107*
DOI: https://doi.org/10.12989/sem.2017.64.1.093

Vibro-acoustic analysis of un-baffled curved composite panels with experimental validation

Nitin Sharma[1a], Trupti R. Mahapatra[*1] and Subrata K. Panda[2b]

[1]*School of Mechanical Engineering, KIIT University, Bhubaneswar 751024, Odisha, India*
[2]*Department of Mechanical Engineering, NIT Rourkela, 769008, Odisha, India*

(Received April 29, 2017, Revised July 15, 2017, Accepted July 16, 2017)

Abstract. The article presents the vibration and acoustic responses of un-baffled doubly curved laminated composite panel structure under the excitation of a harmonic point load. The structural responses are obtained using a simulation model via ANSYS including the effect various geometries (cylindrical, elliptical, spherical and hyperboloid). Initially, the model has been established by solving adequate number of available examples to show the convergence and comparison behaviour of the natural frequencies. Further, the acoustic responses are obtained using an indirect boundary element approach for the coupled fluid-structure analysis in LMS Virtual.lab by importing the natural frequency values. Subsequently, the values for the sound power level are computed using the present numerical model and compared with that of the available published results and in-house experimentally obtained data. Further, the acoustic responses (mean-square velocity, radiation efficiency and sound power level) of the doubly curved layered structures are evaluated using the current simulation model via several numerical experimentations for different structural parameters and corresponding discussions are provided in detail.

Keywords: composite doubly curved panels; acoustic radiation; indirect boundary element method; sound pressure level; radiated sound power; experimental analysis

1. Introduction

Curved panels of different geometrical form made up of dissimilar materials (conventional and advanced) are widely used as the structural components (automotive, submarine hull, the fuselage of an airplane etc.) due to their inherent advantages. In general, these components have excellent load bearing capacity, shock resistant ability including the certain resistance to the acoustic radiation emission. The sound radiation from any vibrating structure is influenced by several factors such as the dynamic properties of the vibrating structure, support conditions, surrounding fluid and types of load (mechanical, thermal and aerodynamic) during their operational life. Therefore, a holistic design approach is highly essential to estimate the necessary influence of aforementioned factors which makes the design process more challenging. Every now and then different techniques have been proposed and implemented for the evaluation of the frequency and acoustic responses of vibrating isotropic and laminated composite structures (Bui *et al.* 2011, Zhang *et al.* 2017). The mechanical structural responses (vibration, bending and buckling) are significantly influenced by the choice of the mid-plane theories based on which laminated panels are modelled to derive the equations of motion. The classical laminated plate theory (CLPT), first-order shear deformation theory (FSDT) (Yin *et al.* 2014, Yu *et al.* 2016), the higher-order shear deformation theory (HSDT) (Belabed *et al.* 2014, Mahi *et al.* 2015, Yahia *al.* 2015, Bouderba *et al.* 2016, Bellifa *et al.* 2016, Yin *et al.* 2016, Liu *et al.* 2017, Chikh *et al.* 2017) and various refined higher-order kinematics (Tounsi *et al.* 2013, Zidia *et al.* 2014, Beldjelili *et al.* 2016, Bennoun *et al.* 2016, Draiche *et al.* 2016) are favorably employed by many researchers specifically during the analysis of laminated composite structures. Several techniques for studying the wave propagation in functionally graded laminates have also been proposed (Golub *et al.* 2012, Hedayatrasa *et al.* 2014, Boukhari *et al.* 2016). It is well known that the acoustic radiation of any structure largely depends on the vibration frequency and it may vary according to the medium in which the structure vibrates. Additionally, the surrounding medium exerts a load on the structure which in turn alters the response characteristics including the acoustic emissions of the structure. Therefore, the coupling between the surrounding medium and the structure needs to be sensibly considered while determining the acoustic responses numerically.

Usually, the structural problems are modelled and solved using the finite element method (FEM) in association with the existing well-defined solution techniques. Similarly, the surrounding medium is considered to be infinite and modelled via boundary element method (BEM) for the solution purpose. The surface nodes of the finite element (FE) mesh of the structure is assumed to coincide with the nodes of the

∗Corresponding author, Associate Professor
E-mail: trmahapatrafme@kiit.ac.in
[a]Faculty Research Scholar
E-mail: nits.iiit@gmail.com
[b]Assistant Professor
E-mail: call2subrat@gmail.com

 ISSN: 1225-4568 (Print), 1598-6217 (Online)

boundary mesh of the domain. Subsequently, to establish the coupling between the structure and the fluid, the classical Helmholtz wave equation is discretized over the boundary in association with the FE mesh. The coupled FEM/BEM problem for any structure vibrating in an external medium have been widely studied and several formulations and/or methodologies have been reported in the past (Ben and Hamdi 1987, Everstine and Henderson 1990, Jeans and Mathews 1990). Johnson and Cunefare (2002) performed structural acoustic optimization of the composite cylindrical shell subjected to an external monopole source using FEM/BEM technique by minimizing the sum of squared pressure amplitudes. Further, the effect of curvature ratio on the sound radiation of the baffled cylindrical panel is investigated by Graham (1995) by considering the surface to be a flat surface and the acoustic field to be outside the cylinder. Similarly, various studies have been reported for the acoustic radiation under on-surface loading from the cylindrical shell. In this regard, the far field acoustic radiation from cylindrical shell subjected to on-surface forces is reported by Guo (1994) using the asymptotic type of analysis. Further, the vibration and acoustic behaviour of the hollow cylinders made up of functionally graded material (FGM) excited on-surface by harmonic mechanical drives in the far-field is investigated via 3D elasticity theory by Hasheminejad and Savadkoohi (2010). Wang and Lai (2000) presented analytical results for the radiation efficiency of thick cylindrical shell structure under mechanical excitation and demonstrated its dependence on the mode of vibration, geometry and the end condition. Wu *et al.* (1999) proposed a novel theoretical model for the analysis of acoustic radiation of a fluid loaded isotropic cylindrical shell subjected to rotating point load. Li *et al.* (2014) performed a coupled analysis based on Flugge's shell theory in conjunction with Helmholtz equation to study the far-field sound radiation from a submerged cylindrical shell at a finite depth from the free surface. Subsequently, the effect of thermal environment on the vibroacoustic responses of a circular isotropic cylindrical shell has been investigated by Jeyaraj *et al.* (2011). Later, the vibration and acoustic radiation characteristics of a baffled orthotropic composite cylindrical shell under the combined hygroscopic environment are reported by Zhao *et al.* (2015). The acoustic radiation from flat and doubly curved fibre reinforced stiffened composite structure have been investigated in details considering different design factors. Cao and Hua (2012) studied theoretically the sound radiation from the shear deformable stiffened laminated composite plate with multiple compliant layers. The acoustic radiation from the shear deformable laminated composite stiffened cylindrical shell (doubly periodic rings and sparse cross stiffeners) panel have also been analysed in much detail (Cao *et al.* 2012, Cao *et al.* 2013). Subsequently, a novel theoretical approach has been employed by Mellow and Karkkainen (2008) for the evaluation of far field sound radiation from the shallow spherical shell in an infinite baffle. Likewise, the spatially distributed transient load effect on the sound radiation values of a submerged spherical shell panel has also been studied (Zakout 2001, Bahari and Popplewell 2015). The sound radiation from a submerged hollow FGM sphere under the action of an axisymmetric distributed internal pressure force has been investigated by Hasheminejad *et al.* (2011) using the linear theory of elasticity. Xiongwei *et al.* (2011) used the hybrid FEM including the statistical energy to study the vibration and acoustic responses of the clamped reinforced conical shell panel under the thermal environment. The complex structural configurations such as aircraft body, submarine hull are mostly combinations of single/doubly curved panel components. Hence, the analytical results for the vibration and the acoustics responses of the submarine hull of different geometries (cylindrical shell closed by truncated conical shells and circular plate) under the harmonic excitation are reported by Caresta and Kessissoglou (2010) by using the coupled FEM/BEM technique. Also, the modal models of the stiffened and un-stiffened fluid loaded structures (plate and shell) have been presented in past (Herwig *et al.* 2013, Li 2011) to assess the vibration and acoustic responses accurately. The acoustic analysis has also been performed to predict the desired responses for the fluid-loaded multi-layered shells of revolution (Qu and Meng 2015) and FG shells of revolution (Qu and Meng 2016). Attempts have also been made to investigate the sound radiation behaviour of the fibre reinforced composite flat panels as they are favourably used in stringed musical instruments because of their superior damping and noise reduction ability (Damodaran *et al.* 2015, Liu *et al.* 2015). Subsequently, the effect of structural properties, source conditions and factors influencing the sound transmission through the laminated composite cylindrical shells immersed in an external fluid in context of a flying aircraft is investigated analytically by Daneshjou *et al.* (2007) The active control of acoustic radiations from the laminated composite and FG structures by incorporating piezoelectric layers are investigated (Cao *et al.* 2013, Hasheminejad *et al.* 2013) via the FSDT and 3D piezo-elasticity theories.

The comprehensive review clearly indicates that studies on the vibroacoustic responses of the curved (cylindrical, spherical, elliptical and hyperboloid) shell panel made of isotropic/composite (laminated composite, FGM, sandwich) materials under the influence different loading (stationary harmonic point load and surface force) including the unlike environments (thermal and hygroscopic) are very few in numbers. Additionally, we note that the effect of the geometrical parameters (geometrical configurations, aspect ratios, thickness ratios, curvature ratios, lamination schemes) and support conditions including the type and location of excitation on the vibro-acoustic behaviour of the doubly curved laminated composite panel structure (specifically with unequal curvature) are not reported in the open literature. Hence, the present research aims to investigate the vibroacoustic responses of the un-baffled laminated single as well as the double curvature shell panels numerically by considering other important geometrical design parameters. For the analysis purpose, a customized simulation model in ANSYS environment has been developed via batch input technique (ANSYS parametric design language, APDL code). Further, the structural acoustic responses are computed with the help of LMS

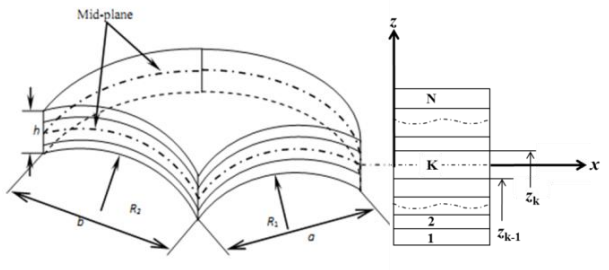

Fig. 1 Geometry and lamination scheme of laminated composite doubly curved shell panels

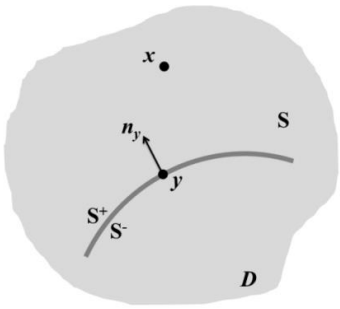

Fig. 2 Un-baffled doubly curved shell panel in acoustic medium

Virtual.Lab using the simulated frequencies as the input parameter. The vibration frequencies of the panel are used to perform the coupled fluid-structure analysis using the indirect boundary element method where the mean square velocity, radiation efficiency, radiated sound power level, and sound pressure level are considered as the acoustic response indicators. Finally, the corresponding numerical experimentations have been performed to evaluate the influence of geometry, end supports, curvature ratios, aspect ratios and thickness ratios on the acoustic responses of various shell panels (cylindrical, spherical, elliptical and hyperboloid) after satisfied comparison (numerical and experimental) and convergence study.

2. Mathematical formulation

A schematic presentation of the geometry of curved shell panel including the lamination schemes chosen for the current analysis are presented in Fig. 1. The curvature parameters, R_1 and R_2 are used to classify the panel geometries i.e., (a) Spherical: R_1=R_2=R, (b) Cylindrical: R_1=R, R_2=∞, (c) Hyperboloid: R_1=+R, R_2=−R, and (d) Elliptical: R_1=R, R_2=2R.

The simulation model of the laminated composite doubly curved shell panels has been developed in ANSYS using APDL code. The panel structure is discretised using the Shell 281 element chosen from ANSYS element library. This element has eight nodes and six degrees of freedom per node. The following displacement field equations are normally adopted to derive the required strain for the evaluation of energy equation and conceded in the following form

$$\begin{aligned} u(x,y,z,t) &= u_0(x,y) + z\theta_x(x,y) \\ v(x,y,z,t) &= v_0(x,y) + z\theta_y(x,y) \\ w(x,y,z,t) &= w_0(x,y) + z\theta_z(x,y) \end{aligned} \tag{1}$$

where, t is the time and the displacements of any general point of the panel structure are presented using u, v and w as the displacement functions along the x, y and z coordinate axes, respectively. Further, u_0, v_0 and w_0 are corresponding displacements of a particular point on the mid-plane. Similarly, θ_x and θ_y are the rotations of normal to the mid-surface (z=0) about the y and x- axes, respectively; θ_z is the higher order term in the Taylor series expansion which accounts for the linear variation of displacement function along the thickness direction. Now, the modal analysis is performed and the in-vacuo modes of the vibrating structure can be obtained by solving the generalized eigenvalue equation and conceded to the following form

$$([K]-\omega^2[M])\{\Phi\} = 0 \tag{2}$$

where, [K] and [M] are the system stiffness and mass matrices, respectively. In addition, ω is the natural frequency of vibration and {Φ} is the corresponding mode shape vector. Further, the computed mode shapes and the natural frequencies of each mode are employed for the coupled vibroacoustic analysis to evaluate the acoustic responses of the panel structure. For the analysis purpose a coupled FEM/BEM approach is adopted and indirect boundary element is used for modelling the fluid medium.

The acoustic responses are computed by solving the well-known Helmholtz wave equation as conceded in the following line

$$\nabla^2 p + k^2 p = 0 \quad \text{in D} \tag{3}$$

where, k=ω/c is the wave number, p is the acoustic pressure, ω is the angular frequency, c is the speed of sound in the surrounding acoustic medium D. Fig. 2 shows an un-baffled vibrating thin doubly curved shell panel having fluid on both sides.

The surface of the panel is represented as the union of its two separate sides S^+ and S^- and $S = S^+ \cup S^-$, where superscript '+' indicates the positive side defined the outward normal vector at the surface S^+, and the negative superscript '−' indicates the opposite side, i.e., S^-. The acoustic variables are modelled in the form of potentials, namely the single layer potential (σ) and the double layer potential (μ) which is related to the acoustic pressure and velocity jumps across the surface S and expressed in the following forms

$$\sigma = \frac{\partial p^+}{\partial n} - \frac{\partial p^-}{\partial n} \tag{4}$$

and

$$\mu = p^+ - p^- \tag{5}$$

The solution to the Helmholtz wave equation in the form of potentials defined as in Eqs. (4) and (5) can be obtained as in Eq. (6) (Nowak and Zieliński 2015)

$$p_x = -\int_S [G_{xy}\sigma_y - \frac{\partial G_{xy}}{\partial n_y}\mu_y]dS_y \ , \quad \forall x \notin S \text{ and } y \in S \tag{6}$$

where, G is the free space green's function defined as

$$G_{xy} = \frac{1}{4\pi|x-y|}e^{-jk|x-y|} \tag{7}$$

where, $|x-y|$ is the distance between the source point y and the field point x.

$$\sigma = 0 \text{ , and } \left.\frac{\partial p}{\partial n}\right|_y = -j\omega\rho V_n \quad \text{for} \quad y \in S \tag{8}$$

Let V_n be the normal component of velocity of the structure. After imposing the Neumann boundary condition on the surface of the structure, given by Eq. (8), Eq. (6) is re-written as Eq. (9)

$$-j\omega\rho V_n = \int_S \mu_y \frac{\partial^2 G_{xy}}{\partial n_x \partial n_y} dS_y \tag{9}$$

The Eq. (9) is solved for unknown potential μ defined on the surface S. The solution to the integral equation is obtained by minimizing the functional J defined as (Cao *et al.* 2013)

$$J = 2\int_S j\omega\rho\mu_x V_{n,y} + \int_S\int_S \mu_x\mu_y \frac{\partial^2 G_{xy}}{\partial n_x \partial n_y} dS_x dS_y \tag{10}$$

The second integral in Eq. (10) is rewritten by using the properties of green's function G and the continuity of μ over S as the following (Tournour and Atalla 1998)

$$\begin{aligned}&\int_S\int_S \mu_x\mu_y \frac{\partial^2 G_{xy}}{\partial n_x \partial n_y} dS_x dS_y \\ &= \int_S\int_S G_{xy}[k^2\mu_x\mu_y(n_x \cdot n_y) - (\nabla\times\mu_x)\cdot(\nabla\times\mu_y)]dS_x dS_y \\ &= \langle\mu\rangle[D(\omega)]\{\mu\}\end{aligned} \tag{11}$$

and

$$\int_S j\omega\rho\mu_x V_{n,y} = \langle U\rangle[C]\{\mu\} \tag{12}$$

where, U is the degree of freedom vector of the structure. Therefore, a coupled equation representing structure and acoustic medium is obtained as

$$\begin{pmatrix} K + i\omega Q - \omega^2 M & C \\ C^T & -\frac{1}{\rho\omega^2}D(\omega) \end{pmatrix} \begin{Bmatrix} U \\ \mu \end{Bmatrix} = \begin{Bmatrix} F \\ 0 \end{Bmatrix} \tag{13}$$

where, Q is the damping matrix and F is the external load vector. The system is symmetric, frequency dependent and full. The Eq.(13) is solved for U and μ. The sound power (W_{rad}) radiated by the vibrating shell panel is given by

$$W_{rad} = \frac{\omega^2}{2}\langle U^*\rangle \text{real}[Z(\omega)]\{U\} \tag{14}$$

where, $Z(\omega)$ is defined as the acoustic radiation impedance given by Eq. (15)

$$Z(\omega) = -j\rho\omega CD(\omega)^{-1}C^T \tag{15}$$

The radiated sound power level is defined as

$$\text{Sound Power Level} = 10\times\log\left(\frac{W_{rad}}{W_{ref}}\right) \tag{16}$$

where, W_{ref} is the reference power equal to 10^{-12} W. The normal mean square velocity ($\langle v_n^2\rangle$) on the surface S can be defined as

$$\langle v_n^2\rangle(\omega) = \frac{1}{2S}\int_S |V_n^2| dS \tag{17}$$

The radiation efficiency (Ω) is a measure of the ability of the structure to radiate sound and is defined as

$$\Omega = \frac{W_{rad}}{\rho c S\langle v_n^2\rangle} \tag{18}$$

The sound pressure level (SPL) at a field point is defined as

$$\text{SPL}=20\times\log\left(\frac{p}{p_{ref}}\right) \tag{19}$$

where, p is the pressure at the field point and p_{ref} is the reference pressure equal to 20 μPa.

3. Methodology

The doubly curved shell panel model is developed in ANSYS (in framework of FSDT mid-plane kinematics) using APDL code. The Shell 281 iso-parametric element from ANSYS library is used to discretize the model. The modal analysis is performed after imposing appropriate support conditions and the natural frequencies and the mode shapes are obtained.

The various support conditions considered in the present analysis to reduce the number of unknowns are as follows:

1. All edges clamped boundary condition (*CCCC*):

$u_0 = v_0 = w_0 = \theta_x = \theta_y = \theta_z = 0$ at x=0 and a; y=0 and b.

2. All edges simply supported boundary condition (*SSSS*):

$v_0 = w_0 = \theta_y = \theta_z = 0$ at x=0 and a;

$u_0 = w_0 = \theta_x = \theta_z = 0$ at y=0 and b.

3. All edges hinged boundary condition (*HHHH*)

$u_0 = v_0 = w_0 = \theta_y = \theta_z = 0$ at x=0 and a;

$u_0 = v_0 = w_0 = \theta_x = \theta_z = 0$ at y=0 and b.

The ANSYS results file as obtained (*.rst* extension) containing the modal data is imported into LMS Virtual.Lab environment for computing the acoustic response. In LMS Virtual.Lab, an indirect BEM approach is adopted for obtaining the coupled responses. The loads are attached to the appropriate nodes, a field mesh representing the microphone locations is defined in the fluid domain for obtaining the acoustic responses and the problem is solved.

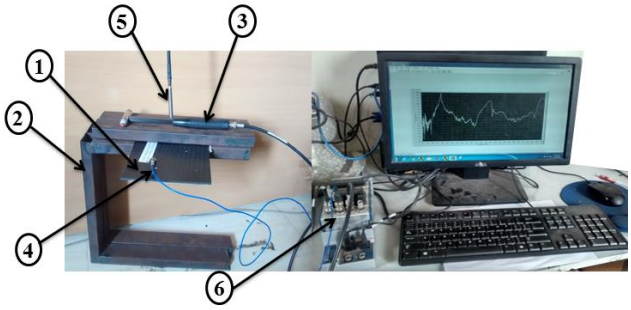

Fig. 3 Experimental setup for measuring natural frequencies and sound pressure level of cantilever laminated composite flat panels: (1). Laminated composite plate, (2). Fixture, (3). Impact hammer, (4). Accelerometer, (5). Microphone, (6). NI PXIe 1071

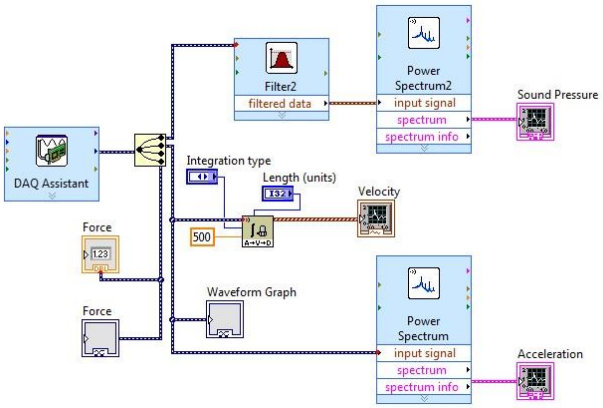

Fig. 4 Diagram of circuit designed in LABVIEW to record vibration and acoustic response of laminated flat panels

The results for radiated sound power, radiation efficiency, mean square velocity and sound pressure at the field point are exported for further analysis.

The presently computed frequency responses and radiated sound power values are compared with those of the published numerical results. In addition, the numerically obtained values of the natural frequencies at different modes and the SPLs are compared with present experimental results. The detailed experimental plan is depicted in the following section.

4. Experimental analysis

A lab scale experimental set-up has been developed at National Institute of Technology Rourkela (NIT, Rourkela), Odisha, India to obtain the free vibration (modal analysis) and acoustic responses of laminated composite flat panels. Two different laminated composites namely, six layered woven $[0°/90°]_3$ glass/epoxy and four layered symmetric angle-ply $[\pm 45°]_s$ carbon/epoxy plates are fabricated using conventional hand lay-up technique. In order to obtain their mechanical properties, specimens are prepared in accordance with ASTM standard (D790) and a tensile test has been performed using the universal testing machine (UTM-INSTRON 1195) available at NIT, Rourkela, Odisha, India. The experimentally obtained material properties of the glass/epoxy and carbon/epoxy plates are listed in Table 1 and denoted as M1 and M2, respectively.

Fig. 3 depicts the present experimental set-up used for recording the natural frequencies and SPLs of the vibrating plate under cantilever (*CFFF*) support condition. The plate (1) is clamped along one edge using the fixture (2). The impact hammer (3) is used to excite the plate at a particular location on the plate, the signals generated are captured by the accelerometer (4), and the pressure in the surrounding medium is recorded by microphone (5).

The accelerometer and the microphone are interfaced with LABVIEW through PXIe-1071 (6) that receives analogue voltage signal, uses an inbuilt AD (analogue to digital) converter to transform it into the digital signal form. Further, the digital signal is processed through LABVIEW software. The block diagram of the circuit designed in LABVIEW to process the signals is presented in Fig. 4.

5. Results and discussion

The free vibration and acoustic response of doubly curved laminated composite panels subjected to harmonic point load have been obtained using ANSYS and LMS Virtual.Lab, respectively. The model is tested for convergence for different geometries and support conditions and the free vibration results as well as the acoustic radiation results are validated with the results in the published literature and subsequent experimental results. This is essential to establish the accuracy of the model and to build confidence in its efficacy in predicting the vibro-acoustic response of curved panels.

The effect of various structural parameters namely, curvature ratio (R/a), aspect ratio (a/b), thickness ratio (a/h) and lamination scheme on the acoustic response parameters (mean square velocity, radiation efficiency, radiated sound power) of doubly curved laminated composite structures for different support conditions (*SSSS*, *CCCC*, *HHHH*, *CFFF*, *FFFF* and *CSCS*) have been investigated. The materials used in the parametric study are listed in Table 1. The panels are excited by a harmonic point load of 1N at the central node of the structures and the sound pressure level (SPL) is measure at a location 0.1m above the central node in the fluid medium. A modal damping of 1% is considered throughout the analysis.

5.1 Convergence and validation studies

The convergence behaviour of the present model is checked by computing the non-dimensional frequency for different mesh divisions and simultaneously comparing them with the existing results. The natural frequencies are further compared with the experimentally obtained values. The acoustic parameters are validated by comparing the sound power level obtained using the present scheme with the existing results in the published literature. In order to build more confidence on the model, the sound pressure level at point in the fluid domain obtained using the present model is compared with the experimentally obtained values.

Table 1 Materials used in experiments and in the parametric study

	Glass/Epoxy Material: M1	Carbon/Epoxy Material: M2	Material: M3 (Chakravorty *et al.* 1996, Reddy and Liu 1985)	Material: M4 (Zhao *et al.* 2013)
E_1	7.205×10^9 Pa	6.469×10^9 Pa	$25\times E_2$	1.725×10^{11} Pa
$E_2= E_3$	6.327×10^9 Pa	5.626×10^9 Pa	1	6.9×10^9 Pa
$\nu_{12}= \nu_{23}= \nu_{13}$	0.17	0.3	0.25	0.25
$G_{12}= G_{13}$	2.8×10^9 Pa	2.05×10^9 Pa	$0.5\times E_2$	3.45×10^9 Pa
G_{23}	1.4×10^9 Pa	1.025×10^9 Pa	$0.2\times E_2$	1.725×10^9 Pa
ρ	1420.05 kg/m^3	1388 kg/m^3	1	1600 kg/m^3

Table 2 Convergence and validation of non-dimensional frequency of clamped laminated composite doubly curved spherical, elliptical and hyperboloid shell panels

Mesh size	Spherical R_x/R_y =1	Elliptical R_x/R_y =0.5	Hyperboloid R_x/R_y =-1
	0°/90°/0°	0°/90°/0°	0°/90°/0°
2×2	96.046	72.713	94.531
4×4	85.203	59.801	83.877
6×6	81.413	55.603	79.885
8×8	81.054	55.194	79.521
10×10	80.991	55.129	79.464
12×12	80.973	55.111	79.445
14×14	80.966	55.105	79.439
16×16	80.960	55.102	79.439
Chakravorty *et al.* (1996)	81.409	56	79.841

5.1.1 Convergence and validation of natural frequency

The convergence behaviour and the free vibration response represented by non-dimensional frequency parameters is tested and presented. Doubly curved laminated composite shell panels (spherical, elliptical and hyperboloid) under *CCCC* boundary conditions as taken by Chakravorty *et al.* (1986) and laminated composite cylindrical panels under *SSSS* boundary conditions as taken by Reddy and Liu (1985) with M3 material properties (Table 1) are considered. The convergence behaviour the non-dimensional natural frequency ($\varpi = \omega a^2/h\sqrt{\rho/E_2}$, where ω is the natural frequency in rad/s) and its validation with the considered reference values is established. Table 2 shows the first non-dimensional frequency for different mesh sizes corresponding to two lamination schemes for each of the geometries. Table 3 shows the first non-dimensional frequency for cylindrical shell panels for ratios. The results from the literature are also provided for the comparison purpose. It is clear from the results that the model converges well with the mesh refinement corresponding to different curvature. The present values of the non-dimensional frequencies are in excellent agreement with the reference results. Based on convergence study, a (12×12) mesh has been used for computation purpose throughout the analysis.

5.1.2 Experimental validation of natural frequency

Experiments have been conducted to acquire the freevibration responses of six layered woven glass/epoxy plate (material M1) with a=0.15 m, b=0.15 m, h=0.002 m and four layered symmetric angle-ply $[\pm45^o]_s$ carbon/epoxy laminated plate (material M2) with a=0.15 m, b=0.15 m, h=0.00375 m using a lab scale experimental set-up as described in Section 3. The material properties of the specimens are provided in Table 1. The natural frequencies are obtained from the experiments for first five modes under CFFF boundary condition and shown in Table 4 along with the results computed using the current simulation model. It is evident from both the convergence and comparison study that the present numerical results are in good agreement with established numerical values and present experimental results as well. The differences between the numerical and the experimentally obtained values can be attributed to the limitation in applying the perfect displacement boundary conditions on the plate as it is very difficult to replicate the exact conditions for multiple tests of the same specimen. It is clear from the discussion in this and the previous sub-sections that the present model produces reliable results so far as the free vibration responses of the doubly curved laminated composite structures are concerned. In the following sub-section, the acoustic radiation from the vibrating structures is computed using coupled FEM/BEM approach in LMS Virtual.Lab environment. The sound power level obtained using the present numerical model is compared to and validated with the results in the available literature. Further, the sound pressure level (SPL) computed using the present numerical scheme at a point in the fluid domain is also validated with the values obtained from the lab scale experiments.

5.1.3 Numerical validation of sound power level

A rectangular isotropic plate with the following properties, a=0.455 m, b=0.379 m young's modulus, E=2.1×10^{11} Pa, Poisson's ratio, ν=0.3 and density, ρ=7850 kg/m^3 under *SSSS* boundary condition as taken by Li and Li (2008) is chosen for the numerical validation of sound power radiated by the plate. A constant damping ratio of 0.01 is considered for the analysis. Fig. 5 shows the sound power level computed using the present formulation compared with the reference values. It can be clearly seen that the current values closely follow the reference values over the entire range of frequency under consideration.

The difference is attributed to the fact that FSDT, used

Table 3 Convergence and validation of non-dimensional frequency of simply supported laminated composite cylindrical shell panels

	Reddy and Liu (1985)		Present					
			Mesh size					
R/*a*	FSDT	HSDT	2×2	4×4	6×6	8×8	10×10	12×12
5	20.361	20.36	21.265	20.405	20.381	20.38	20.379	20.379
10	16.634	16.63	17.216	16.638	16.622	16.622	16.621	16.621
20	15.559	15.55	16.039	15.555	15.541	15.541	15.541	15.541
50	15.245	15.23	15.693	15.237	15.225	15.225	15.225	15.225
100	15.199	15.19	15.643	15.191	15.179	15.179	15.179	15.179

Table 4 Experimental validations of the natural frequencies of six layered woven glass/epoxy composite flat panel (M1) and four layered symmetric angle-ply carbon/epoxy flat panel (M2) under CFFF boundary condition

Mode	Natural Frequency (Hz)					
	Material: M1			Material: M2		
	Present Experimental	Present Numerical	% diff.	Present Experimental	Present Numerical	% diff.
1.	28	31.7163	11.717	62.5	56.1837	-11.242
2.	68	81.1288	16.183	152	141.395	-7.500
3.	164	200.376	18.154	378	344.199	-9.820
4.	234	250.49	6.583	485	445.274	-8.922
5.	267	293.153	8.921	561	510.393	-9.915

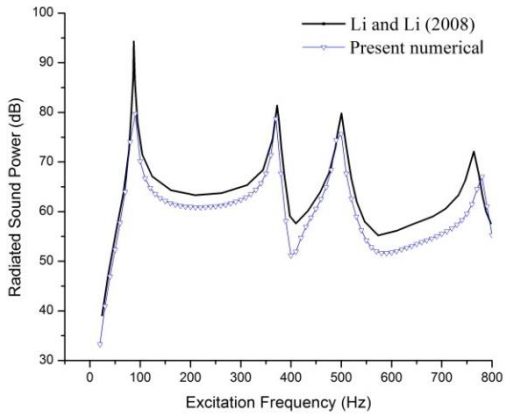

Fig. 5 Validation of sound power level

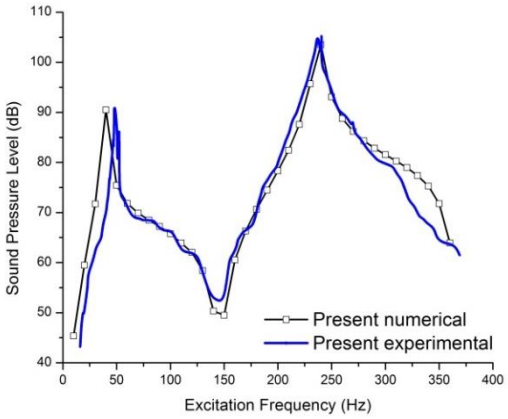

Fig. 6 Experimental validation of sound pressure level

to model the structure, over estimates the frequencies thereby giving relatively less nodal displacements which in turn causes lower acoustic radiation as compared to the reference.

5.1.4 Experimental validation of sound pressure level

The sound pressure level of a rectangular orthotropic plate of material M2 with a=0.15 m, b=0.18 m, h=0.00375 m under *CFFF* boundary condition is obtained experimentally and compared to the values obtained numerically. The comparison is shown in Fig. 6. It can clearly be observed that the values obtained numerically follow the experimental values closely except for certain regions. The overall trend followed by the two is similar. The difference in the values is due to the fact that the displacement boundary conditions are difficult to be imposed in the experiments. Also, the accuracy of the damping model chosen for the numerical analysis leads to the differences between the two results.

5.2 Numerical illustrations

In this section, an extensive parametric study on the acoustic response of the doubly curved laminated composite shell panels is presented. The properties of composite material M4 have been utilized for the computation purpose, if not stated otherwise. The mean square velocity, radiation efficiency and sound power level of the vibrating shell panel is taken as the acoustic response indicator. Also, the directivity pattern of sound pressure radiated by the first mode of the panels is compared for different configurations. The SPL directivity pattern is obtained for the first natural frequency at points in the surrounding medium lying on a circle of radius 0.3 m centred at a distance of 1 m above the central node of the structure. The shell panels are excited by harmonic point load of 1 N at the central node of the finite

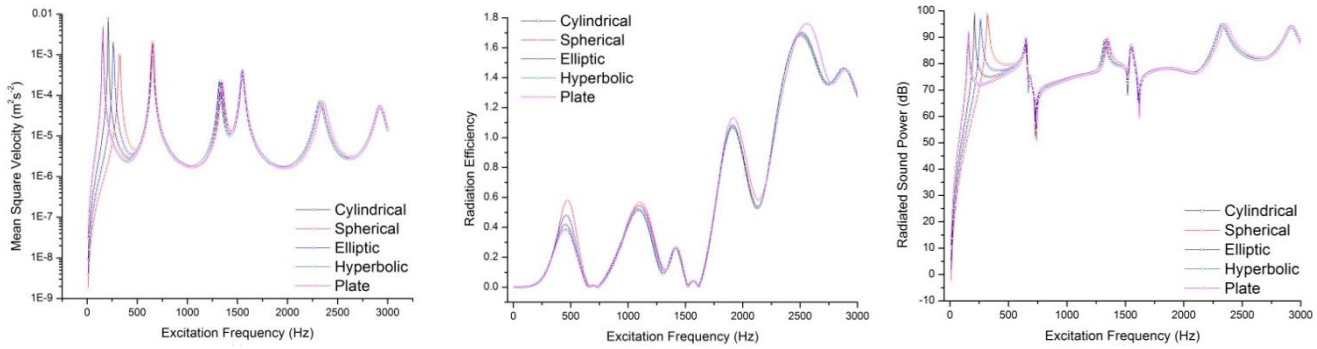

(a) (b) (c)

Fig. 7 Influence of geometry on the (a) Mean square velocity; (b) Radiation efficiency and (c) Radiated sound power of the vibrating laminated composite panels (SSSS, four layered anti-symmetric angle-ply, $(45^o/-45^o)_2$)

element mesh. A modal damping of 1% is considered throughout the analysis. The behaviour of the panels for different conditions is analysed and discussed in detail in the following sub-sections.

5.2.1 Effect of geometry on acoustic indicators

It is well known that the acoustic behaviour of curved panels is different from that of beams and plates due to the curvature effects. The influence of the geometry on the acoustic radiation from the vibrating laminated composite structures is investigated in this example. The geometrical properties of the panels are taken as: a/b=1, a=0.4 m, a/h=100 and R/a=10. Five different geometries namely, cylindrical, spherical, elliptical, hyperboloid and flat plate under *SSSS* boundary condition and anti-symmetric angle-ply $(45^o/-45^o)_2$ lamination scheme are chosen for the analysis. It can clearly be observed from Fig. 7(a), (c) that the acoustic behaviour of the panels is different for first few resonant modes. After the first coincidence frequency of 1503.32 Hz, the panels radiate equally. The average sound power radiated by the panels is maximum for the plate and minimum for the spherical panel, whereas the trend is reversed after the first resonant mode. The radiation efficiency crosses unity only after the first coincidence frequency and the same can be observed from Fig. 7(b).

5.2.2 Effect of aspect ratio

The influence of aspect ratio on the sound power radiated from the cylindrical, spherical, elliptical and hyperboloid laminated composite shell panels $(0^o/0^o/30^o/-30^o)_2$ lamination scheme under *CCCC* boundary condition is investigated and presented in this section. The geometrical properties are taken as: b=0.4 m, a/h=100, R/a=10 and the aspect ratio is varied as a/b=0.5, 1, 1.5 and 2. The variation of sound power radiated by vibrating shell panels with the aspect ratio is shown in Fig. 8 for different geometries. The panels have the first coincidence frequency equal to 1503.32 Hz. It is observed that the first natural frequency is the highest for a/b=0.5 case indicating that the panels are most stiff for the least value for the aspect ratio. Therefore, the first mode is excited at a higher excitation frequency and the sound power level curves for all of the geometries have late first peaks for a/b=0.5 and the same is evident from Fig. 8. All of the geometries emit maximum average acoustic radiation for a/b=0.5 after the occurrence of the first resonance peak. The radiated sound power generally follows a decreasing trend with increasing a/b ratio for all geometries. Fig. 9 shows the SPL directivity pattern for the first resonant mode for different a/b corresponding to the considered geometries. The patterns resemble monopole distribution as the (1,1) mode radiates sound normal to the panels. It is clear that for the values of aspect ratio greater than unity, the SPL is the highest for the hyperboloid, followed in decreasing order by spherical, cylindrical and elliptical panel. Also, the average SPL is lesser for a/b=2 case compared to a/b=1.5 case for all of the geometries. The spherical panel radiates maximum sound pressure for $a/b\leq1$. The cylindrical and elliptical geometries radiate equally for a/b=0.5. This behaviour can be attributed to the less curvature along the y-direction (R_2=2R) that resembles the straight edge of the cylindrical panel.

5.2.3 Effect of support conditions

This section presents the effect of support conditions on the acoustic radiation from doubly curved laminated composite panels. The panels are considered to be formed of 4 layered symmetric angle ply with $(45^o/-45^o)_s$ lamination scheme. The geometrical properties are taken as: a/b=1, b=0.4 m, a/h=100 and R/a=10. The acoustic radiation from all the geometries is analysed for five sets of support conditions namely, *SSSS*, *CCCC*, *FFFF*, *CFFF*, and *HHHH*. The coincidence frequency of the panels is equal to 1503.32 Hz. It can be observed from Fig. 10 that the acoustic radiation from the panels is greatly influenced by the support conditions. It can be seen that for all of the geometries, the behaviour of panels is similar for *CFFF* and *FFFF* boundary conditions with the more power being radiated for *CFFF* case as compared to the *FFFF* case. It is also clear that the *CCCC* case radiates more sound after first resonance frequency compared to the other boundary conditions in case of all of the geometries. In all of the geometries, the *SSSS* case radiates more than the *HHHH* case until the excitation frequency of first mode is reached. The behaviour of the geometries for these two cases is almost identical after the first depression on the curve (around 600 Hz for both of these geometries). It is also observed that there is no significant variation in the radiated sound power with geometry for each support condition after

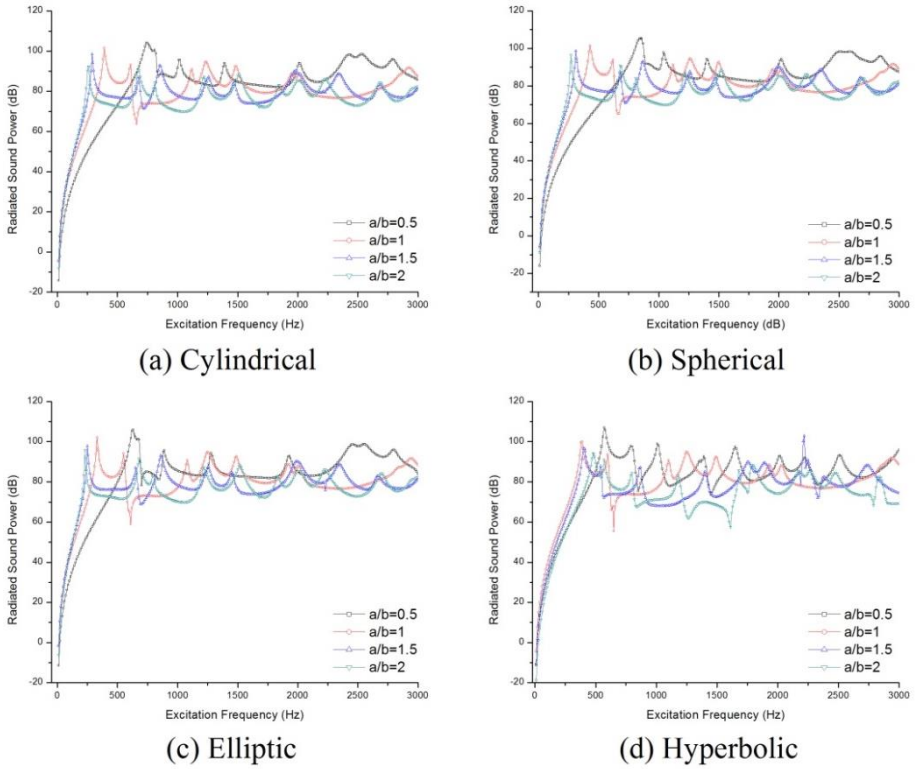

Fig. 8 Influence of aspect ratio on sound power radiated by doubly curved panels (*CCCC*, (0°/0°/30°/ 30°)2): (a) Cylindrical, (b) Spherical, (c) Elliptical and (d) Hyperboloid

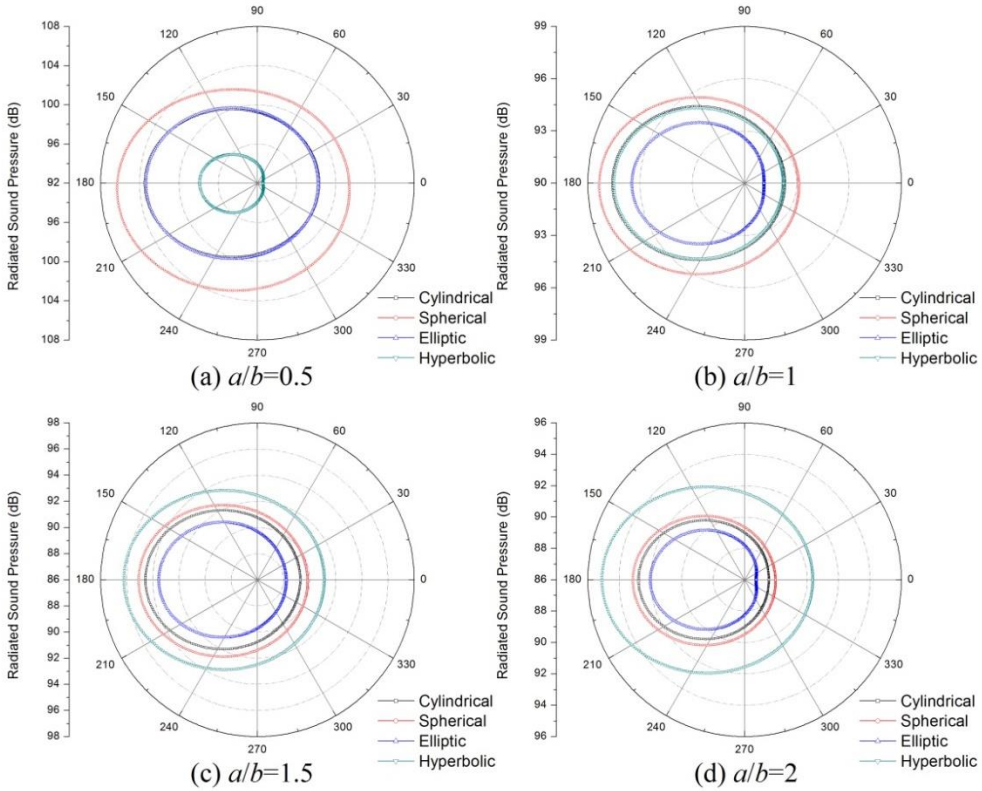

Fig. 9 Directivity patterns of sound pressure radiated by doubly curved panels (*CCCC*, $(0°/0°/30°/ 30°)_2$) for different aspect ratios: (a) a/b=0.5, (b) a/b=1, (c) a/b=1.5 and (d) a/b=2

the first coincidence frequency.

5.2.4 Effect of thickness ratio

In this section, the influence of thickness ratio on the

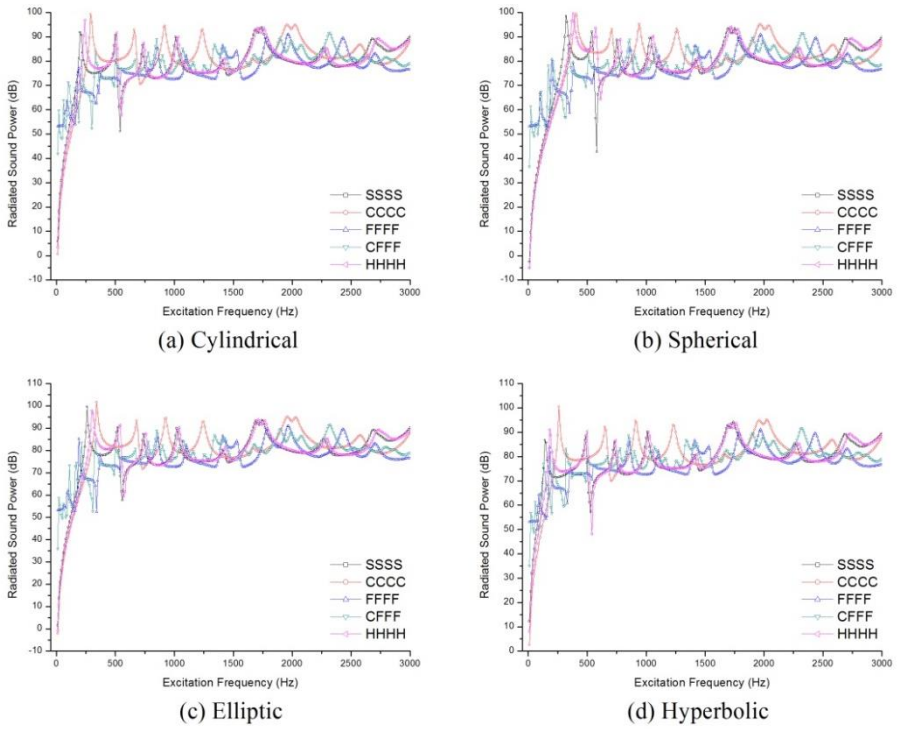

Fig. 10 Influence of support conditions on sound power radiated by doubly curved panels ($(45^o/\ 45^o)_s$): (a) Cylindrical, (b) Spherical, (c) Elliptical and (d) Hyperboloid

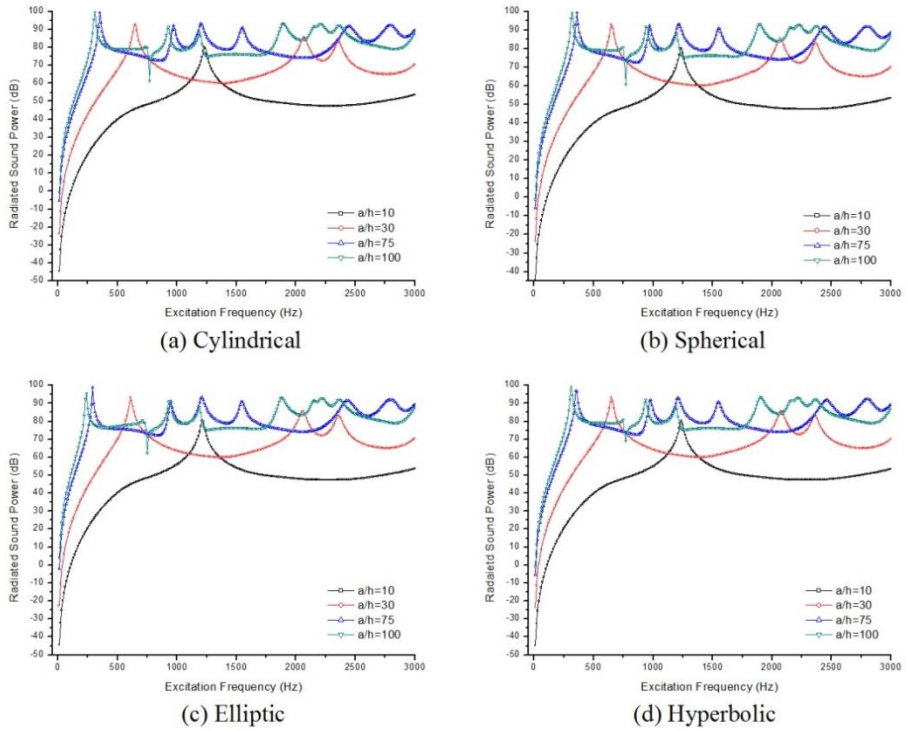

Fig. 11 Influence of thickness ratio on sound power radiated by doubly curved panels (*CSCS*, $(0^o/90^o)_2$): (a) Cylindrical, (b) Spherical, (c) Elliptical and (d) Hyperboloid

sound radiation characteristics of doubly curved laminated composite shell panels under *CSCS* boundary condition is investigated. Four layered anti-symmetric cross-ply panels with $(0^o/90^o)_2$ lamination scheme are considered. The geometrical properties are taken as: a/b=1, b=0.4 m, R/a=10 and thickness ratio is varied as a/h=10, 30, 75 and 100. The first coincidence frequencies for increasing value of aspect ratio are (150.33, 450.99, 1127.5, and 1503.3) Hz. The sound power radiated by different geometries for varying aspect ratio is shown in Fig. 11. It is observed from Fig. 10

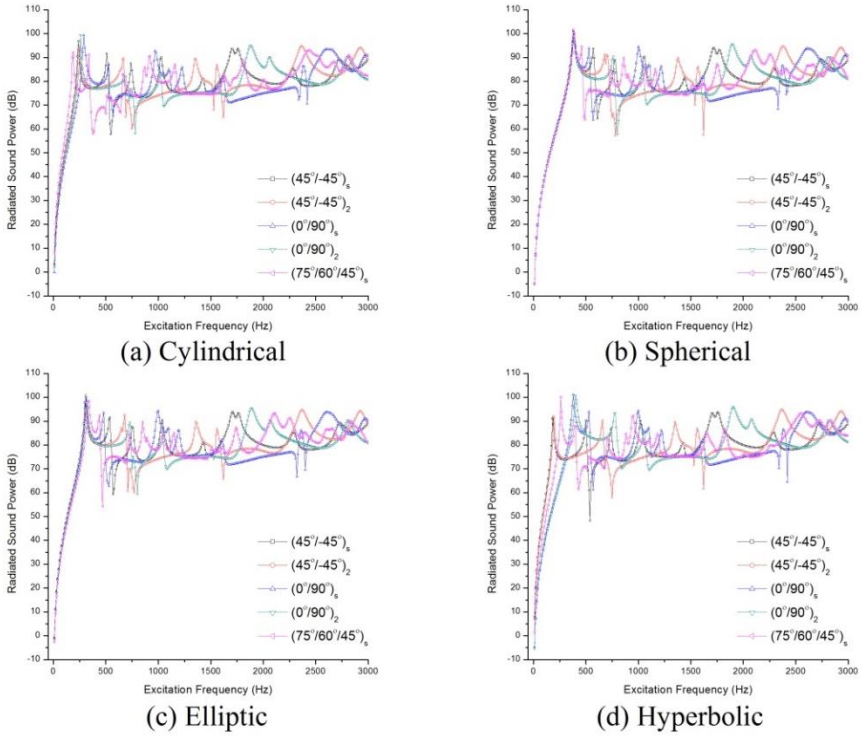

Fig. 12 Influence of lamination scheme on sound power radiated by doubly curved panels (*HHHH*): (a) Cylindrical, (b) Spherical, (c) Elliptical and (d) Hyperboloid

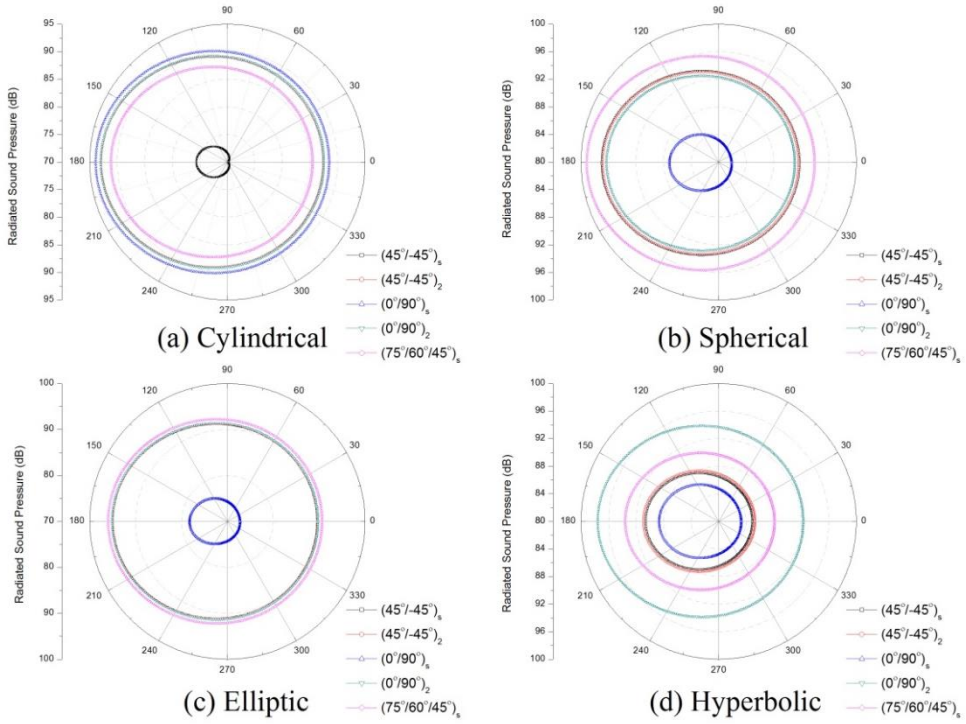

Fig. 13 Directivity patterns of sound pressure radiated by doubly curved panels (*HHHH*): (a) Cylindrical, (b) Spherical, (c) Elliptical and (d) Hyperboloid

that the sound power radiated by panels follow an increasing trend with increasing a/h ratio throughout the frequency range under consideration for all of the geometries. As a/h increases, the shell panels (R/a=10) become increasingly thin and tend to radiate more sound. The behaviour is true for all geometries with the a/h=10 being the least radiating and a/h=100 being the most radiating case.

5.2.5 Effect of lamination scheme

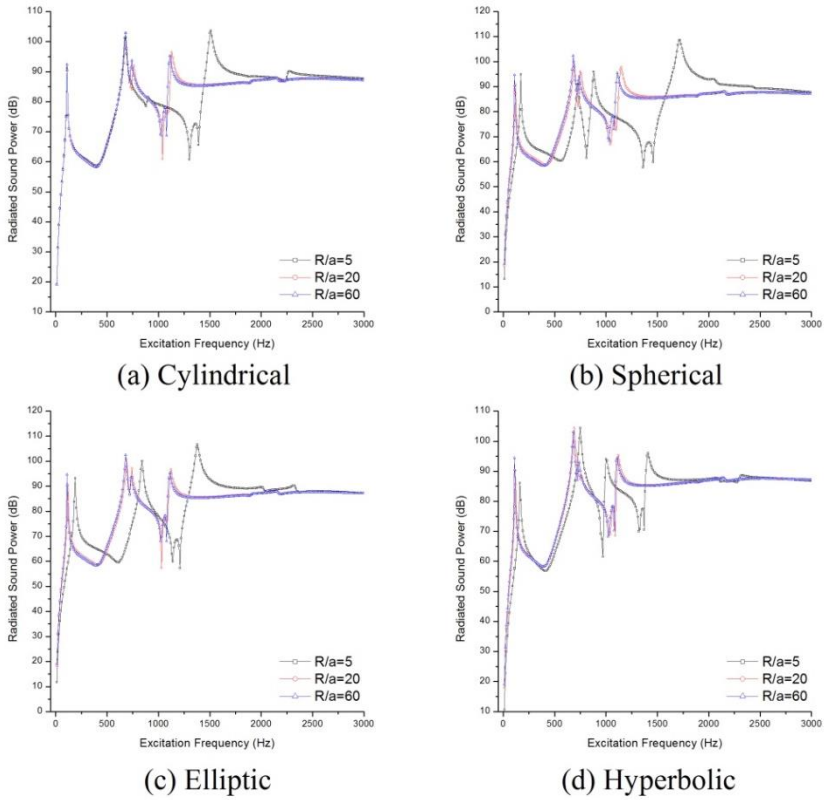

Fig. 14 Influence of curvature ratio on sound power radiated by doubly curved panels (*CFFF*, $(0^o/90^o)_2$): (a) Cylindrical, (b) Spherical, (c) Elliptical and (d) Hyperboloid

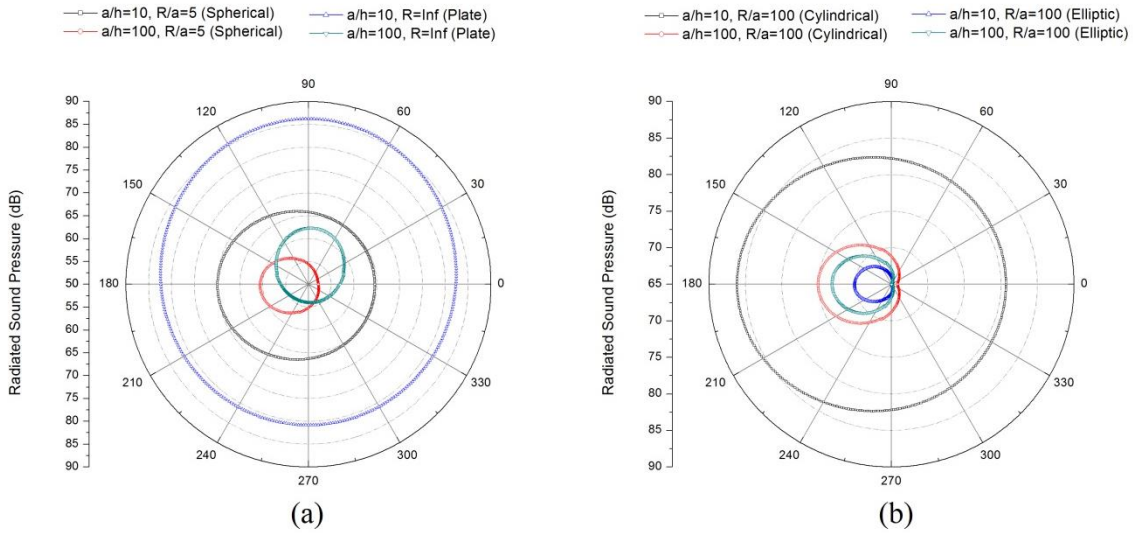

Fig. 15 Comparison of directivity patterns for different geometries (*CFFF*, $(0^o/90^o)_2$): (a) *R*/*a*=5, (b) *R*/*a*=100

In this example, laminated composite doubly curved shell panels (*a*/*b*=1, *b*=0.4 m, *R*/*a*=10 and *a*/*h*=100) under *HHHH* boundary condition are considered. The effect of five lamination schemes namely, symmetric angle-ply $(\pm 45^o)_s$, anti-symmetric angle-ply $(\pm 45^o)_2$, symmetric cross-ply $(0^o/90^o)_s$, anti-symmetric cross ply $(0^o/90^o)_2$ and symmetric hybrid $(75^o/60^o/45^o)_s$ on the radiated sound power and SPL directivity is investigated and shown in Fig. 12 and Fig. 13, respectively. It is observed from Fig. 12(b) and (c) that all of the lamination schemes radiate equally up to the excitation frequency of first mode in the case of spherical and elliptical case. However, the first resonance peaks for different schemes tend to distribute over a range of frequency (100 Hz-200 Hz) for cylindrical panels and (200 Hz-400 Hz) for hyperboloid shell panels, thereby leading to difference in the radiation characteristics. The $(0^o/90^o)_s$ scheme radiates the least average sound power and has the least fluctuations in the radiation after the first coincidence frequency. Fig. 13 shows the SPL directivity plots for different schemes corresponding to the first

resonant frequency. It is clear that the $(0°/90°)_s$ scheme radiates the least sound pressure in all geometries other than cylindrical in which the $(\pm 45°)_s$ scheme radiates the least. It is interesting to note that the symmetric and anti-symmetric angle ply have near identical sound pressure radiation for all of the geometries.

5.2.6 Effect of curvature ratio

Finally, the influence of curvature ratio on the acoustic radiation characteristic of laminated composite doubly curved shell panels under *CFFF* boundary conditions is investigated and presented in this section. Anti-symmetric $(0°/90°)_2$ lamination scheme is considered with the geometrical properties a/b=1, b=0.1 m, a/h=100 and curvature ratio varied as R/a=5, 20, and 60. Radiated sound power level for different geometries with varying curvature ratio is plotted and shown in Fig. 14. A quick observation of the results reveals that the sound power levels converge to a common value after first coincidence frequency for all of the geometries. However, the acoustic radiation behaviour is considerably different for different curvature ratios for the frequencies less than the coincidence frequency. As the value of R/a increases, the shell panels become increasingly shallow and the curves of sound power level for $R/a \geq 20$ almost resemble each other. This behaviour is observed in the case of all geometries under consideration. The sound pressure radiated by different geometries is compared for shallow and deep shells and shown in Fig. 15. The comparison between deep spherical panel (R/a=5) and flat panel (R=∞) for a/h=10, 100 (corresponding to thick, thin shell panels, respectively) is shown in Fig. 15(a). It is clear that the values of SPL corresponding to the same thickness ratio are smaller for spherical panel as compared to flat panel. On similar lines, the SPL for shallow (R/a=100) cylindrical and elliptical panels are compared and shown in Fig. 15(b). It can be observed that the elliptical panel causes lesser SPL compared to the cylindrical panel for each value of the thickness ratio. It is interesting to note that the pressure values are the least for thin cylindrical, spherical and flat panels irrespective of the curvature ratio which is in direct contrast with elliptical panels.

6. Conclusions

The influence of support conditions, geometry, curvature ratio, aspect ratio, thickness ratio and lamination scheme on the vibration and acoustic response of un-baffled laminated composite cylindrical, spherical, elliptical and hyperboloid shell panels has been investigated and discussed in detail. The free vibration responses (modal analysis) are computed using numerical model in ANSYS using APDL code. Coupled vibroacoustic analysis has been performed in LMS Virtual.Lab environment using an indirect BEM formulation by importing the results of modal analysis. The free vibration responses obtained numerically are compared with the results in the published literature and present experimentally obtained values to establish the validity of the model. The sound power level, chosen as one of the acoustic response indicators, is computed using the present formulation and validated with the results available in the published literature. Further, lab scale experiments are performed to obtain the SPL at point in the fluid medium due to the vibrating flat panel and the numerically obtained SPL is validated with the experimental values. The average SPL is lesser for a/b=2 irrespective of geometries. The sound power radiated by panels follows an increasing trend with increasing thickness ratio. The hybrid scheme causes maximum pressure in the surrounding medium in case of spherical and elliptical geometries.

References

Bahari, A. and Popplewell, N. (2015), "Comment on 'transient response of an acoustic medium by an excited submerged spherical shell' (*J. Acoust. Soc. Am*., **109**(6), 2789-2796 (2001)) (L)", *J. Acoust. Soc. Am.*, **137**(5), 2966-2969.

Belabed, Z., Houari, M.S.A., Tounsi, A., Mahmoud, S.R. and Beg, O.A. (2014), "An efficient and simple higher order shear and normal deformation theory for functionally graded material (FGM) plates", *Compos. Part B*, **60**, 274-283.

Beldjelili, Y., Tounsi, A. and Mahmoud, S.R. (2016), "Hygro-thermo-mechanical bending of S-FGM plates resting on variable elastic foundations using a four-variable trigonometric plate theory", *Smart Struct. Syst.*, **18**(4), 755-786.

Bellifa, H., Benrahou, K.H., Hadji, L., Houari, M.S.A. and Tounsi, A. (2016), "Bending and free vibration analysis of functionally graded plates using a simple shear deformation theory and the concept the neutral surface position", *J. Braz. Soc. Mech. Sci. Eng.*, **38**(1), 265-275.

Bennoun, M., Houari, M.S.A. and Tounsi, A. (2016), "A novel five variable refined plate theory for vibration analysis of functionally graded sandwich plates", *Mech. Adv. Mater. Struct.*, **23**, 423-431.

Bouderba, B., Houari, M.S.A., Tounsi, A. and Mahmoud, S.R. (2016), "Thermal stability of functionally graded sandwich plates using a simple shear deformation theory", *Struct. Eng. Mech.*, **58**(3), 397-422.

Boukhari, A., Atmane, H.A., Tounsi, A., Bedia, E.A.A. and Mahmoud, S.R. (2016), "An efficient shear deformation theory for wave propagation of functionally graded material plates", *Struct. Eng. Mech.*, **57**, 837-859.

Bui, T.Q., Nguyen, M.N. and Zhang, C. (2011), "An efficient meshfree method for vibration analysis of laminated composite plates", *Comput. Mech*., **48**, 175-193.

Cao, X. and Hua, H. (2012), "Sound radiation from shear deformable stiffened laminated plates with multiple compliant layers", *J. Vib. Acoust.*, **134**(5), 051001-051001-12.

Cao, X., Hua, H. and Ma C. (2012), "Acoustic radiation from shear deformable stiffened laminated cylindrical shells", *J. Sound Vib*., **331**(3), 651-670.

Cao, X., Ma, C. and Hua, H. (2013), "Acoustic radiation from thick laminated cylindrical shells with sparse cross stiffeners", *J. Vib. Acoust.*, **135**(3), 031009-031009-10.

Cao, X.T., Shi, L., Zhang, X.S. and Jiang, G.H. (2013), "Active control of acoustic radiation from laminated cylindrical shells integrated with a piezoelectric layer", *Smart. Mater. Struct.*, **22**(6), 065003.

Caresta, M. and Kessissoglou, N.J. (2010), "Acoustic signature of a submarine hull under harmonic excitation", *Appl. Acoust.*, **71**(1), 17-31.

Chakravorty, D., Bandyopadhyay, J.N. and Sinha, P.K. (1996), "Finite element free vibration analysis of doubly curved laminated composite shells", *J. Sound Vib.*, **191**(4), 491-504.

Chikh, A., Tounsi, A., Hebali, H. and Mahmoud, S.R. (2017),

"Thermal buckling analysis of cross-ply laminated plates using a simplified HSDT", *Smart Struct. Syst.*, **19**(3), 289-297.
Damodaran, A., Lessard, L. and Suresh, B.A. (2015), "An overview of fibre-reinforced composites for musical instrument soundboards", *Acoust. Aust.*, **43**(1), 117-122.
Daneshjou, K., Nouri, A. and Talebitooti, R. (2007), "Sound transmission through laminated composite cylindrical shells using analytical model", *Arch. Appl. Mech.*, **77**(6), 363-379.
Draiche, K., Tounsi, A. and Mahmoud, S.R. (2016), "A refined theory with stretching effect for the flexure analysis of laminated composite plates", *Geomech. Eng.*, **11**(5), 671-690.
Everstine, G.C. and Henderson, F.M. (1990), "Coupled finite element/boundary element approach for fluid–structure interaction", *J. Acoust. Soc. Am.*, **87**(5), 1938.
Golub, M.V., Fomenko, S.I., Bui, T.Q., Zhang, C. and Wang, Y.S. (2012), "Transmission and band gaps of elastic SH waves in functionally graded periodic laminates", *Int. J. Solid. Struct.*, **49**, 344-354.
Graham, W.R. (1995), "The influence of curvature on the sound radiated by vibrating panels", *J. Acoust. Soc. Am.*, **98**(3), 1581-1595.
Guo, Y.P. (1994), "Radiation from cylindrical shells driven by on-surface forces", *J. Acoust. Soc. Am.*, **95**(4), 2014-2021.
Hasheminejad, S.M. and Ahamdi-Savadkoohi, A. (2010), "Vibro-acoustic behavior of a hollow FGM cylinder excited by on-surface mechanical drives", *Compos. Struct.*, **92**(1), 86-96.
Hasheminejad, S.M. and Alaei-Varnosfaderani, M. (2013), "Acoustic radiation and active control from a smart functionally graded submerged hollow cylinder", *J. Vib. Control*, **20**(14), 2202-2220.
Hasheminejad, S.M., Malakooti, S. and Akbarzadeh, H.M. (2011), "Acoustic radiation from a submerged hollow FGM sphere", *Arch. Appl. Mech.*, **81**(12), 1889-902.
Hedayatrasa, S., Bui, T.Q., Zhang, C. and Lim, C.W. (2014), "Numerical modelling of wave propagation in functionally graded materials using time-domain spectral Chebyshev elements", *J. Comput. Phys.*, **258**, 381-404.
Jeans, R.A. and Mathews, I.C. (1990), "Solution of fluid-structure interaction problems using coupled finite element and variational boundary element technique", *J. Acoust. Soc. Am.*, **88**(5), 2459-2466.
Jeyaraj, P., Padmanabhan, C. and Ganesan, N. (2011), "Vibro-acoustic response of a circular isotropic cylindrical shell under a thermal environment", *Int. J. Appl. Mech.*, **3**(03), 525-541.
Johnson, W.M. and Cunefare, K.A. (2002), "Structural acoustic optimization of a composite cylindrical shell using FEM/BEM", *J. Vib. Acoust.*, **124**(3), 410-3.
Li, S. and Li, X. (2008), "The effects of distributed masses on acoustic radiation behavior of plates", *Appl. Acoust.*, **69**(3), 272-279.
Li, T.Y., Miao, Y.Y., Ye, W.B., Zhu, X. and Zhu, X.M. (2014), "Far-field sound radiation of a submerged cylindrical shell at finite depth from the free surface", *J. Acoust. Soc. Am.*, **136**(3), 1054-1064.
Liu, J., Zuo, B. and Gao, W. (2015), "Neural network methods applicable to predict the noise reduction ability of nonwoven sandwich absorbers", *Acoust. Aust.*, **43**(1), 129-133.
Liu, S., Yu, T., Bui, T.Q., Yin, S., Thai, D.K. and Tanaka, S. (2017), "Analysis of functionally graded plates by a simple locking-free quasi-3D hyperbolic plate isogeometric method", *Compos. Part B*, **120**, 182-196.
Mahi, A., Bedia, E.A.A. and Tounsi, A. (2015), "A new hyperbolic shear deformation theory for bending and free vibration analysis of isotropic, functionally graded, sandwich and laminated composite plates", *Appl. Math. Model.*, **39**, 2489-2508.
Mariem, J.B. and Hamdi, M.A. (1987), "A new boundary finite element method for fluid-structure interaction problems", *Int. J. Numer. Meth. Eng.*, **24**, 1251-67.
Mellow, T. and Karkkainen, L. (2008), "On the sound field of a shallow spherical shell in an infinite baffle", *J. Acoust. Soc. Am.*, **123**(4), 1880-1891.
Nowak, L.J. and Zielinski, T.G. (2015), "Determination of the free-field acoustic radiation characteristics of the vibrating plate structures with arbitrary boundary conditions", *J. Vib. Acoust.*, **137**, 051001-1-051001-8.
Peters, H., Kessissoglou, N. and Marburg, S. (2013), "Modal decomposition of exterior acoustic-structure interaction", *J. Acoust. Soc. Am.*, **133**(5), 2668-2677.
Qu, Y. and Meng, G. (2015), "Vibro-acoustic analysis of multilayered shells of revolution based on a general higher-order shear deformable zig-zag theory", *Compos. Struct.*, **134**, 689-707.
Qu, Y. and Meng, G. (2016), "Prediction of acoustic radiation from functionally graded shells of revolution in light and heavy fluids", *J. Sound Vib.*, **376**, 112-113.
Reddy, J.N. and Liu, C.F. (1985), "A higher-order shear deformation theory of laminated elastic shells", *Int. J. Eng. Sci.*, **23**(3), 319-330.
Sheng, L. (2011), "Modal models for vibro-acoustic response analysis of fluid-loaded plates", *J. Vib. Control*, **17**(10), 1540-1546.
Tounsi, A., Houari, M.S.A., Benyoucef, S. and Bedia, E.A.A. (2013), "A refined trigonometric shear deformation theory for thermoelastic bending of functionally graded sandwich plates", *Aerosp. Sci. Tech.*, **24**, 209-220.
Tournour, M. and Atalla, N. (1988), "Vibroacoustic behavior of an elastic box using state-of-the-art FEM-BEM approach", *Noise Control Eng. J.*, **46**(3), 83-90.
Wang, C. and Lai, J.C. (2000), "The sound radiation efficiency of finite length acoustically thick circular cylindrical shells under mechanical excitation I: Theoretical analysis", *J. Sound Vib.*, **232**(2), 431-447.
Wu, C.J., Chen, H.L. and Huang, X.Q. (1999), "Vibroacoustic analysis of a fluid-loaded cylindrical shell excited by a rotating load", *J. Sound Vib.*, **225**(1), 79-94.
Xiongwei, Y., Cheng, W., Yueming, L. and Guirong, Y. (2011), "Vibro-acoustic response of a thermally stressed reinforced conical shell", *Adv. Sci. Lett.*, **4**, 1-5.
Yahia, S.A., Atmane, H.A., Houari, M.S.A. and Tounsi, A. (2015), "Wave propagation in functionally graded plates with porosities using various higher-order shear deformation plate theories", *Struct. Eng. Mech.*, **53**(6), 1143-1165.
Yin, S., Hale, J.S., Yu, T., Bui, T.Q. and Bordas, S.P.A. (2014), "Isogeometric locking-free plate element: A simple first order shear deformation theory for functionally graded plates", *Comput. Struct.*, **118**, 121-138.
Yin, S., Yu, T., Bui, T.Q., Zheng, X. and Tanaka, S. (2016), "In-plane material inhomogeneity of functionally graded plates: A higher-order shear deformation plate isogeometric analysis", *Compos. Part B*, **106**, 273-284.
Yu, T., Yin, S., Bui, T.Q., Xia, S., Tanaka, S. and Hirose, S. (2016), "NURBS-based isogeometric analysis of buckling and free vibration problems for laminated composites plates with complicated cutouts using a new simple FSDT theory and level set method", *Thin Wall. Struct.*, **101**, 141-156.
Zakout, U. (2001), "Transient response of an acoustic medium by an excited submerged spherical shell", *J. Acoust. Soc. Am.*, **109**(6), 2789-2796.
Zhang, C., Curiel-Sosa, J.L. and Bui, T.Q. (2017), "A novel interface constitutive model for prediction of stiffness and strength in 3D braided composites", *Comp. Struct.*, **163**, 32-43.
Zhao, X., Geng, Q. and Li, Y. (2013), "Vibration and acoustic response of an orthotropic composite laminated plate in a hygroscopic environment", *J. Acoust. Soc. Am.*, **133**(3), 1433-

1442.
Zhao, X., Zhang, B. and Li, Y. (2015), "Vibration and acoustic radiation of an orthotropic composite cylindrical shell in a hygroscopic environment", *J. Vib. Control*, **23**(4), 1-20.
Zidia, M., Tounsi, A., Houari, M.S.A., Bedia, E.A.A. and Beg, O.A. (2014), "Bending analysis of FGM plates under hygro-thermo-mechanical loading using a four variable refined plate theory" , *Aerosp. Sci. Tech.*, **34**, 24-34.

PL